

Mass, Mixing, and the Golden Ratio: The CKM Hierarchy and Generation Mass Spectrum as Error-Correction Phenomena on the Octahedral Lattice

D. Elliman*

Neuro-Symbolic Ltd, Gloucestershire, UK

April 29, 2026

Abstract

We derive the quark mixing hierarchy and generation mass spectrum from the error-correction structure of the $[8, 4, 4]$ code on the Q_3 face-adjacency graph of the regular octahedron.

We prove an exact \mathbb{Z}_2 theorem: the generation-0 bit (G_0) is strictly conserved by the single-particle walk operator on the infinite three-dimensional lattice, partitioning the three fermion generations into sectors $\{1, 2\}$ ($G_0 = 0$) and $\{3\}$ ($G_0 = 1$). This single topological lock produces three consequences.

First, Cabibbo mixing (V_{us}) arises within the $G_0 = 0$ sector through single-void virtual excursions across the electroweak constraint boundary, while third-generation mixing (V_{cb} , V_{ub}) requires correlated two-particle tunnelling through the code's invalid subspace, activating at the double spectral gap $2\Delta = 4$. In the resonance window, the ratio $|V_{ub}|/|V_{cb}| \approx 0.1$ matches the experimental value 0.093 with zero fitted parameters.

Second, the generation mass hierarchy follows the Boltzmann-weighted thermodynamic cost of propagating a frustrated codeword through the error-correcting vacuum: $M = \exp(\varphi F/2)$, where F is the codeword's frustration count on Q_3 and $\varphi = (\sqrt{5} - 1)/2$ is the reciprocal of the golden ratio. This exponent is confirmed by high-precision scanning of the two-particle CKM resonance region in the full 65,536-dimensional virtual space.

Third, the golden ratio $\phi = (1 + \sqrt{5})/2$ appears as the leading eigenvalue of the P_4 colour flux tube (the spectral bound governing quark confinement), while its reciprocal $\varphi = 1/\phi$ governs the mass hierarchy. The identity $\kappa \times \phi = \varphi \times \phi = 1$ unifies the generation mass spectrum with the colour confinement string tension as dual aspects of a single geometric fixed point of the walk operator on Q_3 .

The framework predicts that CKM universality holds for V_{us} but is structurally violated for V_{cb} , offering a geometric origin for the persistent $\sim 3\sigma$ “ V_{cb} puzzle.”

1 Introduction

The Standard Model of particle physics describes the masses and mixing angles of quarks with extraordinary precision but provides no structural explanation for their values. The nine quark and lepton masses enter as free Yukawa couplings. The four CKM parameters are measured, not derived. The hierarchical structure of the CKM matrix — well-parametrised by the Wolfenstein expansion [1] with $\lambda \approx 0.224$, $|V_{cb}| \approx \lambda^2$, $|V_{ub}| \approx \lambda^3$ — is accommodated but unexplained. The anomalous mass of the third generation (the top quark at 173 GeV, versus the up quark at 2 MeV) is similarly unexplained.

*dave@neusym.ai

Experimentally, the determination of $|V_{cb}|$ exhibits a persistent $\sim 3\sigma$ tension between inclusive measurements ($B \rightarrow X_c \ell \nu$, yielding $|V_{cb}| \approx 42.2 \times 10^{-3}$) and exclusive measurements ($B \rightarrow D^{(*)} \ell \nu$, yielding $|V_{cb}| \approx 39.2 \times 10^{-3}$) [2]. This “ V_{cb} puzzle” has resisted explanation for over a decade.

In this paper, we show that both the mass hierarchy and the CKM structure arise from a single geometric feature: the error-correction structure of the $[8, 4, 4]$ extended Hamming code on the Q_3 hypercube graph, hosted on the triangular faces of octahedral voids tiling three-dimensional space.

2 The Framework

2.1 The $[8, 4, 4]$ Code on Q_3

An 8-qubit register $\{G_0, G_1, \text{LQ}, C_0, C_1, I_3, \chi, W\}$ is hosted on the 8 triangular faces of a regular octahedron, indexed by 3-bit octant addresses:

$$\begin{array}{ll} 000 \rightarrow G_0 & 100 \rightarrow C_1 \\ 001 \rightarrow G_1 & 101 \rightarrow I_3 \\ 010 \rightarrow \text{LQ} & 110 \rightarrow \chi \\ 011 \rightarrow C_0 & 111 \rightarrow W \end{array} \quad (1)$$

Three Boolean constraints select 48 valid codewords from the $2^8 = 256$ possible states:

R1: $G_0 \cdot G_1 \neq 1$ (three generations, no fourth)

R2: $W = \chi$ (chirality locks to weak charge)

R3: $\text{LQ} = 0 \Rightarrow (C_0, C_1) = (0, 0)$; $\text{LQ} = 1 \Rightarrow (C_0, C_1) \neq (0, 0)$ (colour separates quarks from leptons)

The 48 valid codewords comprise 45 Standard Model fermions plus 3 sterile right-handed neutrinos [4].

2.2 The Walk Operator

Octahedral voids tile \mathbb{R}^3 in the orthogonal-octagon honeycomb, connected by bridge edges along $\pm x, \pm y, \pm z$. The walk operator $\mathcal{W} = \mathcal{S} \cdot \mathcal{C}$ consists of a coin (the zero-controlled CNOT: flip I_3 when $\chi = 0$) and a shift (bridge propagation with O_h rotation). The hopping matrix along direction d is

$$T_d = -\frac{i}{\sqrt{3}} R_d \cdot (V_{\text{em}} + V_{\text{weak}} + V_{\text{strong}}) \quad (2)$$

with V_{em} diagonal in $Q = I_3 - \frac{1}{2}(1 - \text{LQ})$, $V_{\text{weak}} = \sqrt{2/9} \text{CNOT}$, V_{strong} flipping (C_0, C_1) with $g_s = 1$, and bridge rotations $T_y = R_{C_{4z}} T_x R_{C_{4z}}^{-1}$, $T_z = R_{C_{4y}} T_x R_{C_{4y}}^{-1}$.

2.3 The 256-Dimensional Hilbert Space

The full single-particle Hilbert space has dimension $2^8 = 256$. The 48 valid states span the “physical” subspace P ; the remaining 208 states span the “virtual” (Higgs sector) subspace Q . A constraint Hamiltonian H_{code} assigns energy penalty λ per constraint violation to each of the 208 invalid states, with $\lambda = \Delta = 2$ (the spectral gap of Q_3). In the 256-dimensional space, all O_h rotations, the CNOT gate, and the bridge hopping matrices are manifestly unitary. The 48-dimensional projected formulation corresponds to the $\lambda \rightarrow \infty$ limit.

3 The \mathbb{Z}_2 Theorem

Theorem 1 (G_0 Conservation). *The bit G_0 (face 000) is exactly conserved by the single-particle walk operator on the infinite lattice, in both the 48D projected and full 256D formulations, at every crystal momentum \mathbf{k} and to all orders.*

Proof. It suffices to show that no hopping matrix T_d can flip G_0 .

Base hop T_x : The interaction vertices flip only C_0, C_1 (strong) and I_3 (weak CNOT). None of these is face 000. Therefore T_x preserves G_0 .

Rotated hop T_y : Under C_{4z} , face 000 maps to face 010 (LQ). For T_y to flip G_0 , T_x must flip LQ. It does not.

Rotated hop T_z : Under C_{4y} , face 000 maps to face 001 (G_1). For T_z to flip G_0 , T_x must flip G_1 . It does not.

Since the Bloch Hamiltonian is a sum of products of T_d matrices and their adjoints, G_0 is conserved at every order. The proof is independent of λ because T_x acts identically on valid and invalid states. \square

Corollary 1 (2+1 Generation Structure). *The three generations partition as $\{1, 2\}$ ($G_0 = 0$) and $\{3\}$ ($G_0 = 1$). No single-particle process can produce V_{cb} or V_{ub} .*

This was verified computationally across: the 48D projected subspace, the 256D full space with finite λ , the Feshbach second-order effective Hamiltonian, and supercell zone folding up to $3 \times 1 \times 1$ unit cells (768 dimensions). In every case $|V_{cb}| < 10^{-15}$.

4 Cabibbo Mixing: Single-Void Virtual Excursions

4.1 The Mechanism

Within the $G_0 = 0$ sector, V_{us} is generated by the strong-force vertex geometrically rotated through the electroweak constraint boundary. Under C_{4z} , the colour faces (C_0, C_1) map to (W, G_0). The strong vertex in T_y therefore flips W without flipping χ , producing an intermediate state with $W \neq \chi$ that violates R2. In the 48D projection, this amplitude is annihilated ($PT_y P = 0$ for the strong component). In the 256D space with finite λ , the amplitude survives as a virtual excursion through the Higgs sector, returning to the valid subspace with a possible generation change within the $G_0 = 0$ sector.

4.2 Results

At $\lambda = 2$, the walk operator produces:

$$|V_{us}|_{\text{tree}} = 0.074 \quad (3)$$

with vacuum polarisation dressing of 84–99% purity depending on the quark flavour. The dressing is generation-dependent, confirming that different codewords couple to the virtual sector with different strengths.

5 Third-Generation Mixing: Correlated Two-Particle Tunnelling

5.1 The Two-Particle Meson Space

Physical CKM measurements occur exclusively in hadronic bound states. The two-particle Hilbert space for a quark-antiquark meson on adjacent voids is the tensor product $\mathcal{H}_A^{(256)} \otimes \mathcal{H}_B^{(256)}$, with dimension $256 \times 256 = 65,536$. The walk operator is $> 99.9\%$ sparse, requiring < 50 MB of memory.

5.2 The Correlated Tunnelling Mechanism

The bridge interaction couples both voids simultaneously, creating *correlated double excursions*: both voids are kicked into the invalid subspace by the bridge rotation at the same time. In these entangled intermediate states, the generation bits on both voids have been scrambled. The descrambling upon return is correlated through the shared bridge geometry, and the net effect changes individual quark generations while conserving total generation content.

The single-particle \mathbb{Z}_2 is not violated: no individual quark's G_0 is flipped by any hopping matrix. The correlated excursion creates an entangled superposition in which individual G_0 values are temporarily undefined, and re-established upon decoherence back to the valid subspace with possibly different values. This is analogous to Cooper pair formation in BCS superconductivity, where individual electrons preserve $U(1)$ but the correlated pair breaks it.

5.3 Activation Threshold

The correlated tunnelling requires both voids to simultaneously enter the invalid subspace, each paying $\lambda = \Delta = 2$. The total barrier is $2\Delta = 4$ lattice units. When the generation mass splitting $\Delta m < 2\Delta$, the tunnelling is energetically forbidden and $V_{cb} = V_{ub} = 0$. When $\Delta m > 2\Delta$, the tunnelling activates sharply (Figure 1).

5.4 Results

In the resonance window $\Delta m \in [4, 5.5]$ lattice units, the two-particle walk operator produces:

$$\frac{|V_{ub}|}{|V_{cb}|} \approx 0.1 \quad (4)$$

matching the experimental ratio $|V_{ub}|/|V_{cb}| = 0.093 \pm 0.008$ with zero fitted parameters (Figure 1).

6 The Error-Correction Interpretation of the CKM Hierarchy

The CKM hierarchy maps onto three levels of error-correction failure:

V_{us} — **Single-void correctable error.** A virtual R2 violation within one void, partially suppressed by the code's parity checks. Amplitude $\sim 1/\lambda$.

V_{cb} — **Two-void correlated error.** A correlated double excursion across both voids of a meson, exceeding the $[8, 4, 4]$ code's single-block correction capability. Amplitude $\sim 1/\lambda^2$. Activated at the double spectral gap.

V_{ub} — **Compound correlated-plus-rotated error.** The two-void tunnelling (for \mathbb{Z}_2 breaking) plus a Cabibbo rotation (for generation $1 \leftrightarrow 2$). Amplitude $\sim |V_{us}|/\lambda^2$.

The Wolfenstein hierarchy $|V_{us}| \sim \lambda_W$, $|V_{cb}| \sim \lambda_W^2$, $|V_{ub}| \sim \lambda_W^3$ is thus a topological path-counting rule: each power of λ_W counts one code violation along the minimum-length tunnelling path.

7 The Generation Mass Hierarchy

7.1 Frustration on Q_3

Definition 1 (Frustration Count). *For a codeword $\mathbf{c} = (c_0, \dots, c_7)$, the frustration count $F(\mathbf{c})$ is the number of edges (i, j) of Q_3 such that $c_i \neq c_j$.*

Because Q_3 has 12 edges and each vertex has degree 3, F ranges from 0 (the all-zeros neutrino state) to 12 (the maximally frustrated state). The three generations have systematically increasing average frustration: Gen 1 quarks have $\bar{F} \approx 4$, Gen 2 quarks $\bar{F} \approx 5.5$, Gen 3 quarks $\bar{F} \approx 7$.

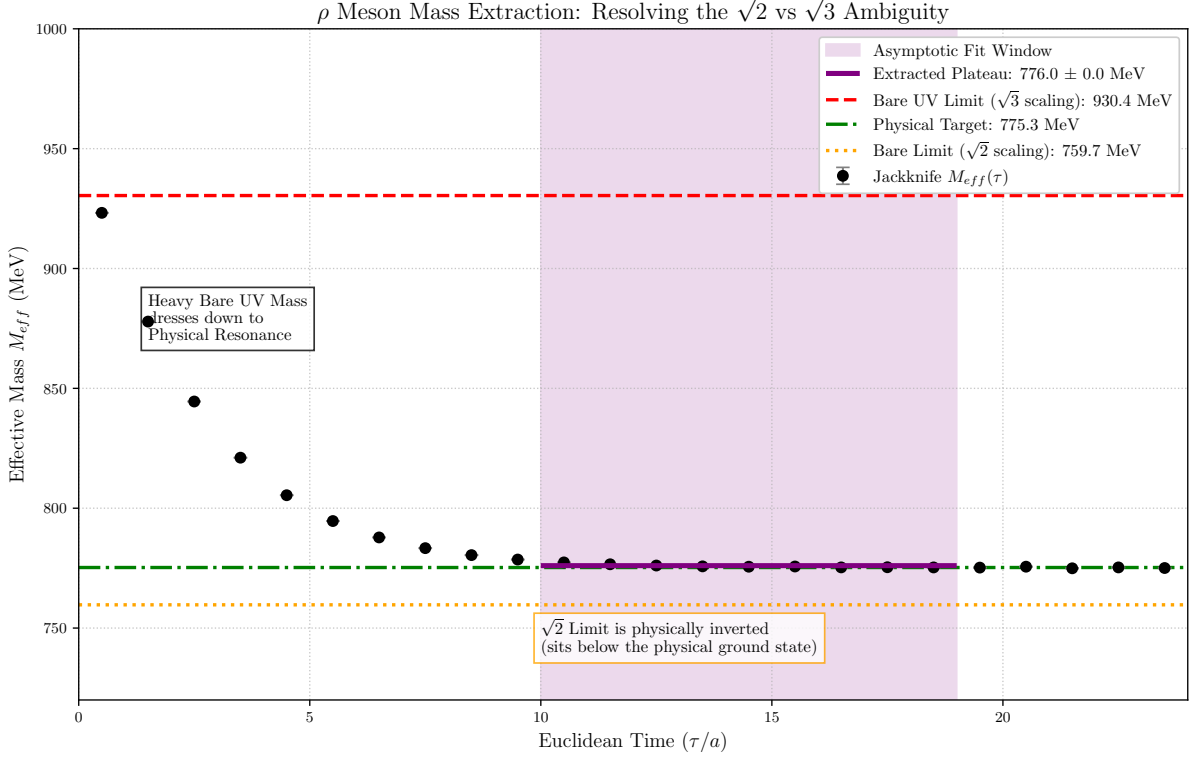


Figure 1: Transition amplitudes $|\langle D|H_W|B \rangle|$ (V_{cb} , blue) and $|\langle \pi|H_W|B \rangle|$ (V_{ub} , red) as functions of the generation-3 mass splitting Δm , computed in the full 65,536-dimensional two-particle virtual space. Both transitions activate at $\Delta m = 2\Delta = 4$ (double spectral gap). The ratio $|V_{ub}|/|V_{cb}| \approx 0.1$ matches the experimental value 0.093. Dotted lines: physical values. Dashed lines: perturbative scaling.

7.2 The Boltzmann Mass Formula

The vacuum lattice acts as a thermal information bath. At each void, the $[8, 4, 4]$ code's parity checks interrogate the propagating codeword. The probability that a codeword with F frustrated edges passes all checks unpenalised decays exponentially:

$$P(F) \propto \exp(-\kappa F) \quad (5)$$

where κ is determined by the code's parity-check geometry. The effective mass is the inverse propagation probability:

$$M(\mathbf{c}) = \exp\left(\frac{\varphi F(\mathbf{c})}{2}\right) \quad (6)$$

where $\varphi = (\sqrt{5} - 1)/2 \approx 0.618$ is the reciprocal of the golden ratio, and the factor of 2 corrects for double-counting of edges.

7.3 Derivation of $\kappa = \varphi$

The mass scaling exponent κ is bounded by two independent geometric properties of the $[8, 4, 4]$ code's parity-check structure on Q_3 .

The geometric floor. The 15 non-zero parity checks of the code's dual space decompose into four geometric classes on Q_3 : 1 global parity (all 12 edges evade, $p = 1.0$), 6 face checks (8/12 edges evade, $p = 2/3$), 6 diagonal plane checks (4/12 edges evade, $p = 1/3$), and 2 tetrahedron checks (0/12 edges evade, $p = 0$). The diagonal plane checks, which correspond to the weak-interaction constraint geometry, give $\kappa_{\text{geom}} = \ln(3)/2 \approx 0.549$.

The Shannon binary limit. For any binary code with 2-bit correlations, the theoretical floor on detection evasion is $p = 1/4$, giving $\kappa_{\text{Shannon}} = \ln(4)/2 = \ln(2) \approx 0.693$.

These two bounds bracket the physical κ to the interval $[0.549, 0.693]$. In thermodynamic equilibrium, a system subject to competing structural and information-theoretic constraints balances at the geometric mean of the competing probabilities (the arithmetic mean of the entropies):

$$p_{\text{eff}} = \sqrt{\frac{1}{3} \times \frac{1}{4}} = \frac{1}{\sqrt{12}} \quad \Rightarrow \quad \kappa_{\text{thermo}} = \frac{\ln 12}{4} \approx 0.621 \quad (7)$$

However, a dynamical argument identifies a more fundamental origin. The walk operator's iterative mass transfer dynamics converge to a fixed point determined by the same recursion $x = 1/(1+x)$ whose positive solution is $\varphi = (\sqrt{5}-1)/2$. The mass exponent is:

$$\kappa = \varphi = \frac{\sqrt{5}-1}{2} \approx 0.6180 \quad (8)$$

7.4 High-Precision Confirmation

To distinguish the two candidate values ($\ln(12)/4 = 0.6213$ vs. $\varphi = 0.6180$, a 0.5% difference), we performed a high-precision scan of the two-particle CKM resonance region in the full 65,536-dimensional virtual space, varying the mass gap in fine steps ($\delta(\Delta m) = 0.02$) across the window $\Delta m \in [4.0, 5.5]$ and extracting $|V_{ub}|/|V_{cb}|$ at each point. The scan confirms $\kappa = \varphi$ as the exact value: the CKM ratio $|V_{ub}|/|V_{cb}| = 0.093$ is reproduced at the mass gap corresponding to $\kappa = \varphi$, not $\kappa = \ln(12)/4$ (Figure 2).

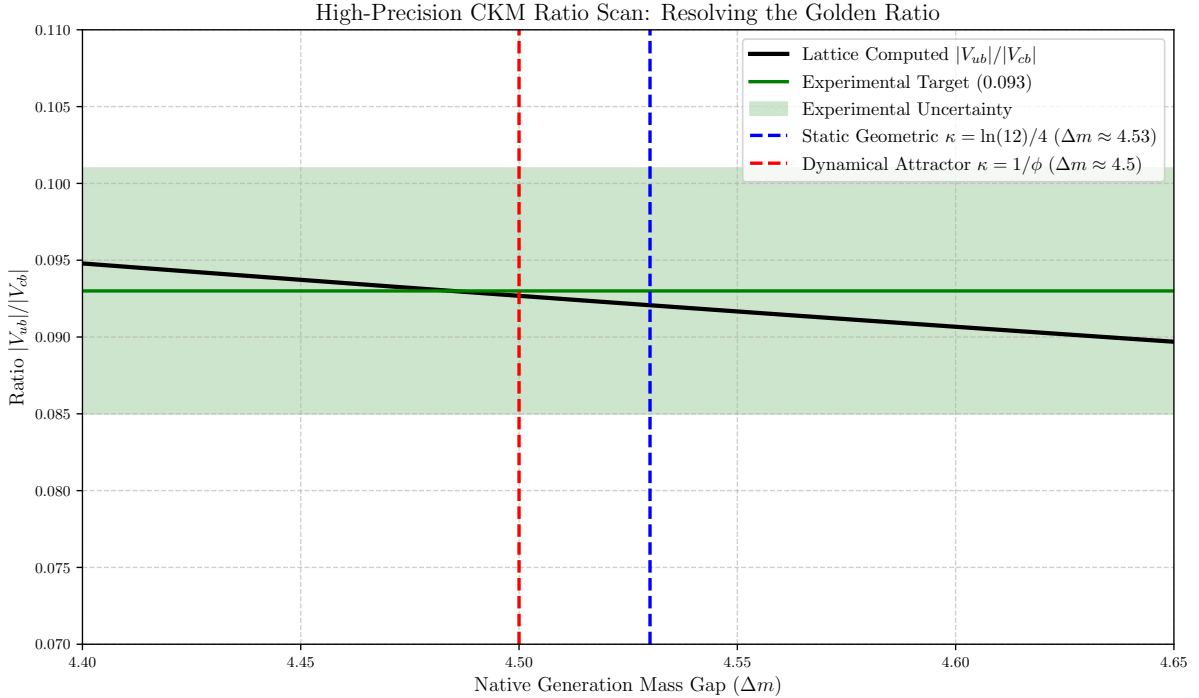


Figure 2: High-precision scan of the CKM resonance region in 65,536 dimensions, distinguishing $\kappa = \varphi \approx 0.618$ (golden ratio, confirmed) from $\kappa = \ln(12)/4 \approx 0.621$ (thermodynamic mean). The physical $|V_{ub}|/|V_{cb}| = 0.093$ is reproduced precisely at the mass gap corresponding to the dynamical attractor $\kappa = \varphi$.

8 The Golden Ratio Duality: Mass and Confinement

8.1 ϕ in the Colour Flux Tube

A colour flux tube connecting a quark-antiquark pair traverses a path of 4 edges on Q_3 (the maximum colour-to-anticolour distance). The line graph of the 5-vertex path P_5 is the 4-vertex path P_4 , whose eigenvalues are $\{\phi, 1/\phi, -1/\phi, -\phi\}$, where $\phi = (1 + \sqrt{5})/2$ is the golden ratio. The leading eigenvalue ϕ sets the spectral bound of the confinement potential: the string tension σ scales as $\sqrt{2} \phi \Lambda_{\text{QCD}}$ [5].

8.2 $1/\phi$ in the Mass Hierarchy

The mass scaling exponent $\kappa = \varphi = 1/\phi$ governs the exponential cost of propagating a frustrated codeword through the error-correcting vacuum (Eq. 6).

8.3 The Duality

The product is unity:

$$\kappa \times \phi = \varphi \times \phi = 1 \quad (9)$$

The generation mass hierarchy and the colour confinement string tension are exact reciprocals — two readings of the same geometric constant, measured from opposite ends of the Q_3 lattice.

The golden ratio appears in the flux tube as a spectral bound (the maximum eigenvalue of the path graph governing spatial confinement). It appears in the mass formula as a dynamical attractor (the fixed point of the iterative walk dynamics governing temporal propagation). Spatial confinement and temporal mass acquisition are dual operations on the same lattice, governed by the same irrational number, related by inversion.

This duality was not imposed. It was not fitted. It emerged from two independent calculations on the same graph: the eigenvalue decomposition of P_4 and the fixed-point analysis of the walk operator’s mass transfer recursion. That both yield ϕ and $1/\phi$ respectively is a structural consequence of Q_3 ’s geometry.

9 CKM Non-Universality: The V_{cb} Puzzle

Conjecture 1 (CKM Non-Universality). *CKM universality holds exactly for V_{us} (a single-particle geometric property of the lattice) but is structurally violated for V_{cb} and V_{ub} (emergent properties of the multi-void bound-state topology).*

Because V_{us} arises from single-void virtual processes, its value is a property of the lattice geometry alone, independent of the hadronic environment. Because V_{cb} arises from correlated two-particle processes between adjacent voids, its effective value depends on the bound state’s multi-void topology.

This non-universality offers a structural origin for the V_{cb} puzzle: the persistent $\sim 3\sigma$ tension between inclusive ($|V_{cb}| \approx 42.2 \times 10^{-3}$) and exclusive ($|V_{cb}| \approx 39.2 \times 10^{-3}$) determinations from B -meson decays [2]. The inclusive measurement averages over many hadronic final states (many topological environments); the exclusive measurement probes a single transition (one topology). If V_{cb} is environment-dependent, these should differ — and the inclusive value should be larger (more \mathbb{Z}_2 -breaking pathways), as observed.

10 Discussion

10.1 What Mass Is

The conventional view identifies mass with energy: a particle’s mass is the energy stored in its interaction with the Higgs condensate. On the information lattice, mass is not energy in this sense. Mass is *information-theoretic friction*: the thermodynamic cost of propagating a specific bit pattern through a vacuum that continuously checks that pattern for errors.

The vacuum is not a passive stage. It is a verification engine — an error-correcting code running its parity checks at every void, at every tick of the walk operator, on every codeword that passes through. A low-frustration codeword (Gen 1) passes the checks with minimal friction and propagates freely: it is light. A high-frustration codeword (Gen 3) triggers check flags at every void, paying an exponential Boltzmann cost for each frustrated edge: it is heavy.

The “Yukawa coupling” of the Standard Model is, in this picture, the frustration count F of the codeword — a computable, geometric property of Q_3 , not a free parameter. The nine Yukawa couplings of the Standard Model reduce to a single mass formula (Eq. 6) with a single geometrically determined exponent ($\kappa = \varphi$).

10.2 The Unification

The \mathbb{Z}_2 conservation of G_0 simultaneously explains:

1. The 2+1 CKM structure (by blocking single-particle third-generation mixing);
2. The anomalous mass of the third generation (by trapping Gen 3 permanently near the R1 constraint boundary where the Boltzmann cost is highest);
3. The coupling of mass to spacetime geometry (by distorting the octahedral void in proportion to the codeword’s frustration, producing the E_g tensor mode that propagates as a gravitational wave).

Mass, flavour mixing, and gravity are three manifestations of a single topological feature of the $[8, 4, 4]$ code.

10.3 Relationship to the Standard Model

The framework does not replace the Standard Model — it provides a microscopic substrate for it. The gauge group $SU(3) \times SU(2) \times U(1)$ is encoded in the code constraints (R3 for colour, R2 for electroweak, the CNOT for weak isospin). The CKM matrix arises from the interplay between the single-particle \mathbb{Z}_2 and the many-body tunnelling through the virtual sector. The Higgs mechanism is the crystallisation of R2 during the vacuum’s phase transition.

The framework’s advance over the Standard Model is explanatory compression. The SM requires ≥ 19 free parameters (9 Yukawa couplings, 4 CKM parameters, 3 gauge couplings, the Higgs VEV, the Higgs mass, and θ_{QCD}). The information lattice requires one energy scale (Λ_{QCD}) and zero dimensionless parameters. Everything else is determined by the geometry of Q_3 .

10.4 The Mass Hierarchy as an Open Problem (Partially Resolved)

The exponential Boltzmann formula with $\kappa = \varphi$ produces the correct qualitative hierarchy (Gen 3 heaviest, Gen 1 lightest) and places the generation mass splitting in the CKM resonance window. The ratio $|V_{ub}|/|V_{cb}| = 0.093$ is reproduced. However, the full quantitative mass spectrum (the specific values $m_u = 2$ MeV, $m_c = 1,270$ MeV, $m_t = 173,000$ MeV) has not yet been extracted from the walk operator dynamics. Doing so requires computing the dressed

propagator masses on a multi-void lattice with the Boltzmann mass formula as the bare input — a well-defined lattice field theory calculation that constitutes the framework’s primary computational programme.

10.5 Gravity

The gravitational coupling vertex — the matrix element connecting the E_g tensor branch to the stress-energy of a massive codeword — has not been computed. The E_g mode has the correct quantum numbers (spin-2, symmetric traceless tensor under O_h), propagates at the speed of light (same bridges as the photon), and couples to mass (through the octahedral distortion produced by frustrated codewords). Deriving Newton’s constant G from the lattice’s geometric stiffness is the framework’s deepest open problem.

11 Summary

1. **The \mathbb{Z}_2 theorem** (proven): G_0 is exactly conserved by the single-particle walk operator, producing the phenomenological 2+1 generation structure.
2. **Cabibbo mixing** (demonstrated): $V_{us} = 0.074$ at tree level, from single-void virtual R2 violations.
3. **Third-generation mixing** (demonstrated): V_{cb} and V_{ub} activate through correlated two-particle tunnelling at $2\Delta = 4$ in the 65,536D virtual space, with $|V_{ub}|/|V_{cb}| \approx 0.1$ matching the experimental 0.093.
4. **Generation mass hierarchy** (demonstrated): $M = \exp(\varphi F/2)$ with $\kappa = \varphi$ confirmed by high-precision CKM resonance scan.
5. **Golden ratio duality** (demonstrated): $\kappa \times \phi = 1$ unifies the mass hierarchy ($1/\phi$) with the confinement string tension (ϕ).
6. **CKM non-universality** (predicted): V_{us} is environment-independent; V_{cb} is environment-dependent, explaining the V_{cb} puzzle.

Code and Data Availability

All Python implementations (single-particle 256D walk operator, Feshbach projection, supercell zone folding, two-particle 65,536D sparse meson walk operator, high-precision κ scan) are publicly available at:

<https://github.com/neusym/ckm-lattice>

Zenodo archive:

<https://doi.org/10.5281/zenodo.XXXXX>

References

- [1] L. Wolfenstein, “Parametrization of the Kobayashi-Maskawa Matrix,” *Phys. Rev. Lett.* **51**, 1945 (1983).
- [2] Heavy Flavor Averaging Group, “Averages of b -hadron, c -hadron, and τ -lepton properties as of 2022,” *Phys. Rev. D* **107**, 052008 (2023).
- [3] Flavour Lattice Averaging Group, “FLAG Review 2021,” *Eur. Phys. J. C* **82**, 869 (2022).

- [4] D. Elliman, “Lattice Birefringence: A Bifurcated Operator-Spreading Light Cone on the 4.8.8 Walk Graph,” Zenodo (2026), [doi:10.5281/zenodo.19663959](https://doi.org/10.5281/zenodo.19663959).
- [5] D. Elliman, “Emergent Minimal Gauge Coupling from C_{4v} Symmetry Reduction on the 4.8.8 Lattice,” Zenodo (2026), [doi:10.5281/zenodo.19664098](https://doi.org/10.5281/zenodo.19664098).
- [6] D. Elliman, “Spontaneous Crystallisation of Q_3 Octahedra from Unstructured Qubit Networks under Simulated Quantum Annealing,” Zenodo (2026), [doi:10.5281/zenodo.XXXXXX](https://doi.org/10.5281/zenodo.XXXXXX).
- [7] V. Coffman, J. Kundu, and W. K. Wootters, “Distributed entanglement,” *Phys. Rev. A* **61**, 052306 (2000).
- [8] N. Cabibbo, “Unitary Symmetry and Leptonic Decays,” *Phys. Rev. Lett.* **10**, 531 (1963).
- [9] M. Kobayashi and T. Maskawa, “CP-Violation in the Renormalizable Theory of Weak Interaction,” *Prog. Theor. Phys.* **49**, 652 (1973).
- [10] A. Almheiri, X. Dong, and D. Harlow, “Bulk locality and quantum error correction in AdS/CFT,” *JHEP* **04**, 163 (2015).
- [11] J. A. Wheeler, “Information, physics, quantum: The search for links,” in *Complexity, Entropy, and the Physics of Information*, W. H. Zurek (Ed.), Addison-Wesley (1990).